

Hierarchical Bayesian Flow Networks for Molecular Graph Generation

Yida Xiong¹, Jiameng Chen¹, Kun Li¹, Hongzhi Zhang¹, Xiantao Cai¹, Wenbin Hu^{1,*}

¹School of Computer Science, Wuhan University, Wuhan, China

*Corresponding author

yidaxiong@whu.edu.cn, jiameng.chen@whu.edu.cn, li_kun@whu.edu.cn, zhanghongzhi@whu.edu.cn, caixiantao@whu.edu.cn, hwb@whu.edu.cn

Abstract

Molecular graph generation is essentially a classification generation problem, aimed at predicting categories of atoms and bonds. Currently, prevailing paradigms such as continuous diffusion models are trained to predict continuous numerical values, treating the training process as a regression task. However, the final generation necessitates a rounding step to convert these predictions back into discrete classification categories, which is intrinsically a classification operation. Given that the rounding operation is not incorporated during training, there exists a significant discrepancy between the model’s training objective and its inference procedure. As a consequence, an excessive emphasis on point-wise precision can lead to overfitting and inefficient learning. This occurs because considerable efforts are devoted to capturing intra-bin variations that are ultimately irrelevant to the discrete nature of the task at hand. Such a flaw results in diminished molecular diversity and constrains the model’s generalization capabilities. To address this fundamental limitation, we propose GraphBFN, a novel hierarchical coarse-to-fine framework based on Bayesian Flow Networks that operates on the parameters of distributions. By innovatively introducing Cumulative Distribution Function, GraphBFN is capable of calculating the probability of selecting the correct category, thereby unifying the training objective with the sampling rounding operation. We demonstrate that our method achieves superior performance and faster generation, setting new state-of-the-art results on the QM9 and ZINC250k molecular graph generation benchmarks.

Introduction

The generative modeling of molecular graphs is a critical yet challenging endeavor in drug discovery (Li et al. 2025a), facilitating the advancement of downstream tasks such as molecular optimization (Zhu et al. 2023; Xiong et al. 2024) and drug target binding affinity prediction (Wu et al. 2024; Li et al. 2025b). Early computational approaches utilizing deep learning attempted to generate molecular graphs in a one-shot manner (Zang and Wang 2020; Kong et al. 2022). However, these methods often struggle to effectively model complex structures. In recent years, diffusion models have demonstrated remarkable performance across various generation tasks (Gong et al. 2024; Chen et al. 2025). These

Copyright © 2026, Association for the Advancement of Artificial Intelligence (www.aaai.org). All rights reserved.

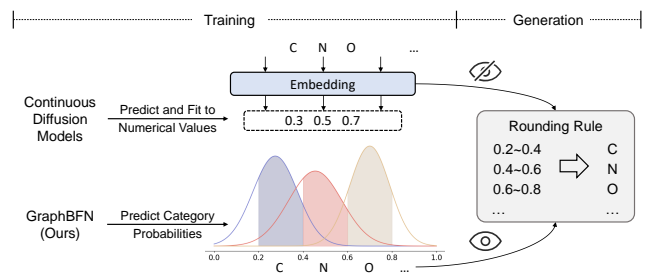


Figure 1: Continuous diffusion models are agnostic of the rounding process in generation and only pursues numerical fitting, while GraphBFN directly calculates the probability of each classification category.

models are generally divided into discrete and continuous types and have been progressively integrated into molecular graph generation task.

Naturally suited for discrete graph structures, discrete diffusion models typically define a forward Markov process that corrupts the graph structure through discrete edits. Conversely, the reverse process learns to restore the graph by framing generation as an iterative classification task (Vignac et al. 2023; Xu et al. 2024). However, these discrete diffusion models sacrifice the smoother representation and dynamic generation inherent in continuous data. Continuous diffusion models have also demonstrated success in this domain (Jo, Lee, and Hwang 2022; Luo, Mo, and Pan 2023). They operate on a continuous representation of a graph, involving a forward noising process that incrementally perturbs this representation with continuous noise while training a core network to reverse this corruption. The primary objective of continuous diffusion models is to predict the numerical values of embedded data within continuous space. Specifically, they aim to minimize regressive error. Nevertheless, during the generation process, these models must perform hard rounding on their predicted continuous values to obtain the final discrete graph. As shown in Fig. 1, it is evident that throughout the entire training phase, these models remain agnostic regarding the rounding rule. Their loss functions are designed to ensure that predicted continuous values closely approximate those prior to noise addition. Furthermore, even minor regressive deviations across

category boundaries can lead to entirely incorrect classification outcomes. Consequently, continuous diffusion models exhibit an inherent limitation when it comes to molecular graph generation.

Recently, Bayesian Flow Networks (BFNs) have been proposed to establish a more effective paradigm for discrete data generation by addressing the limitations of existing methods such as diffusion models (Graves et al. 2023; Song et al. 2024). The primary motivation behind BFNs is to develop a fully continuous and differentiable generative process for the generation of discrete data. The input to BFNs consists of parameters that represent the distribution of data, which is defined by a manually preset prior distribution. During the training process, the Bayesian inference is employed to continuously compute the posterior distribution using observed samples, thereby updating the prior and aligning it more closely with the true data distribution. However, due to all categories being equidistant within the probability simplex, the model cannot progressively approach objectives in a manner akin to that in continuous space (Graves et al. 2023). As a consequence, this results in a convergence process towards data that appears slower and noisier.

To address the aforementioned issues, We propose GraphBFN, a hierarchical BFN framework that reformulates the discrete graph generation problem as a continuous-flow challenge. Rather than assuming equidistance between all discrete categories in the representation space, we map all discrete atom and bond features to a one-dimensional continuous space through a deterministic quantization scheme, facilitating quicker and smoother convergence. Additionally, GraphBFN fully utilizes data distribution parameters by innovatively incorporating Cumulative Distribution Function (CDF) to compute the probabilities of various categories instead of overfitting to specific numerical values. Furthermore, GraphBFN integrates a hierarchical coarse-to-fine scheme by constructing a multi-scale pyramid of graph representations. By generating low-resolution structural scaffolds at coarser levels, GraphBFN effectively capturing both local atomic connectivity and global molecular topology simultaneously, thereby yielding superior molecular graphs. Notably, the training and sampling procedures of GraphBFN are significantly faster than existing methods, which substantially reduces training costs and accelerates the drug discovery process. We summarize our key contributions as follows:

- We introduce the first Bayesian Flow Network for molecular graph generation, which is supervised by hierarchical molecular representations to enhance the effectiveness of the generation process.
- GraphBFN calculates probabilities across various categories rather than fitting to a specific numerical value, thereby unifying the training objective with the sampling rounding operation. The unequal distances between categories also facilitate faster and smoother convergence.
- We demonstrate that GraphBFN achieves state-of-the-art performance on standard molecular graph generation benchmarks while utilizing the minimum number of sampling steps.

Related Work

Generative Models for Molecular Graphs. Deep generative models for molecular graph generation are typically categorized into autoregressive and one-shot models. Autoregressive models generate graphs incrementally, adding nodes and edges in an autoregressive manner (You et al. 2018a,b; Jin, Barzilay, and Jaakkola 2018, 2020). One-shot models based on Variational Autoencoders (VAEs) (Simonovsky and Komodakis 2018), normalizing flow (Zang and Wang 2020; Shi et al. 2020; Luo, Yan, and Ji 2021) and Generative Adversarial Networks (GANs) (De Cao and Kipf 2018; Martinkus et al. 2022) generate the entire graph at once but often struggle with mode collapse, training instability, or producing realistic graph structures.

Diffusion Models for Graph. Inspired by their success in image synthesis, diffusion models have been adapted for molecular graph generation (Liu et al. 2023; Qiu et al. 2023; Li et al. 2024). These models learn to reverse a diffusion process that gradually adds noise to the structure and features of a molecular graph. A key issue lies in how to handle the discrete nature of atom and bond labels. Some methods define a diffusion process directly on the discrete state space (Vignac et al. 2023; Xu et al. 2024), which can be complex to accomplish. Others map discrete attributes to a continuous space and apply standard Gaussian diffusion (Jo, Lee, and Hwang 2022; Huang et al. 2022; Lee, Jo, and Hwang 2023), however, facing the challenge of accurately converting the final continuous output back to discrete labels without information loss.

Bayesian Flow Networks. BFNs (Graves et al. 2023; Song et al. 2024; Qu et al. 2024) are a new type of generative model that learns a mapping between distributions. The process starts with a simple prior distribution and iteratively refines its parameters based on information from the data, which is provided through a sender distribution. A key advantage of BFNs is their ability to create a continuous and differentiable training process for discrete data. The original work achieves this by defining the BFN state as a vector of probabilities on the probability simplex and using multiplicative updates. Our work builds upon the foundational principles of BFNs but proposes a different and simpler mechanism for handling discrete features in the context of molecular graph generation.

Preliminaries

Hierarchically Graph Pooling

A molecular graph \mathcal{G} is defined as $(\mathcal{X}, \mathcal{A})$, where $\mathcal{X} \in \{0, \dots, K_{\mathcal{X}} - 1\}^D$ represents a matrix of D atom features derived from $K_{\mathcal{X}}$ classes, and $\mathcal{A} \in \{0, \dots, K_{\mathcal{A}} - 1\}^{D \times D}$ denotes an adjacency matrix encapsulating bond features from $K_{\mathcal{A}}$ classes.

To obtain hierarchical and multi-scale graph representations, DiffPool (Ying et al. 2018) designs L coarsening layers ϕ_0 that utilize differentiable pooling. Specifically, two graph convolutional networks (GCNs) operate independently to generate a node embedding matrix $Z^{(l)}$ and a node cluster assignment matrix $S^{(l)}$ at l -th coarsening

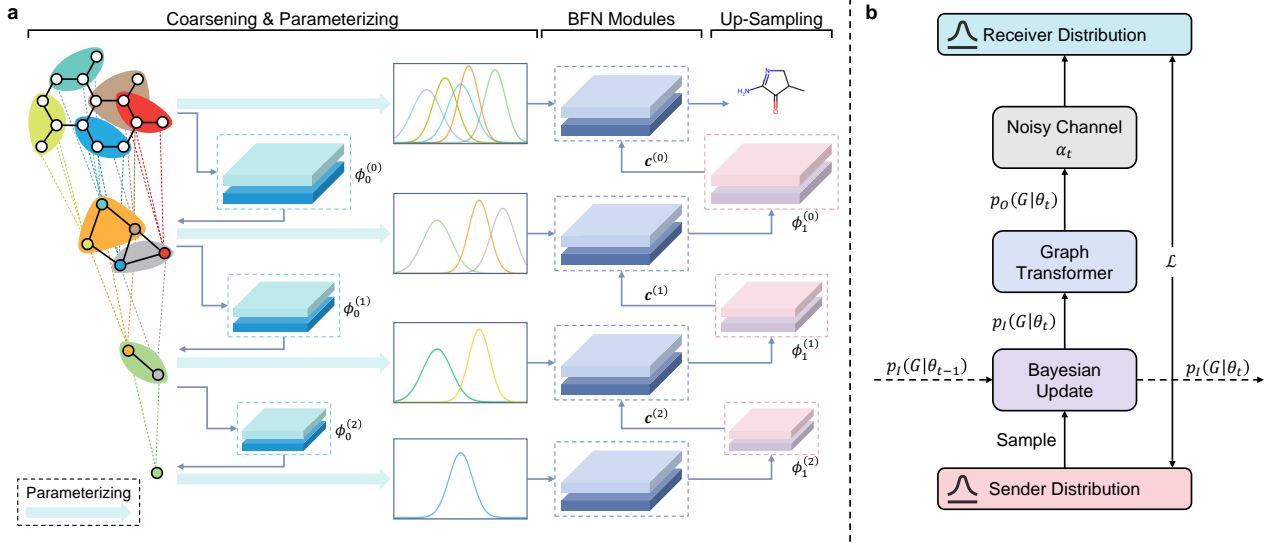


Figure 2: Overall framework of GraphBFN. (a) The original molecular graph is pooled for multi-scale representations, which are subsequently transformed into distribution parameters for each BFN module. Meanwhile, each up-sampling module receives the output from the BFN at a coarser level and generates current condition. (b) The structure of a BFN module at time t .

layer, respectively. Subsequently, the coarsened graph representation $\tilde{G}^{(l+1)} = (\tilde{X}^{(l+1)}, \tilde{A}^{(l+1)})$ is computed via the following equations: $\tilde{X}^{(l+1)} = S^{(l)}{}^T Z^{(l)}$ and $\tilde{A}^{(l+1)} = S^{(l)}{}^T Z^{(l)} S^{(l)}$. This process includes an auxiliary pooling loss to ensure meaningful clusters and is iteratively repeated to create a pyramid of increasingly coarsened graph representations.

Bayesian Flow Networks

The generative process is governed by a set of meticulously defined distributions that evolve over time. This framework can be conceptualized as a data transmission protocol between a "sender" and a "receiver". The receiver utilizes neural networks to predict the noisy data transmitted by the sender.

At any time $t \in [0, 1]$, the model's understanding of a D -dimensional data $\mathbf{x} = (x^{(1)}, \dots, x^{(D)})$ is represented by $\theta = (\theta^{(1)}, \dots, \theta^{(D)})$. These parameters characterize of a factorized *input distribution*:

$$p_I(\mathbf{x}|\theta) = \prod_{d=1}^D p_I(x^{(d)}|\theta^{(d)}). \quad (1)$$

Information is transmitted to the model through noisy messages $\mathbf{y} = (y^{(1)}, \dots, y^{(D)}) \in \mathcal{Y}^D$, which are sampled from the *sender distribution*. This distribution is defined as follows:

$$p_S(\mathbf{y}|\mathbf{x}; \alpha) = \prod_{d=1}^D p_S(y^{(d)}|x^{(d)}; \alpha), \quad (2)$$

where accuracy parameter $\alpha \in \mathbb{R}^+$ regulates the fidelity of the message.

In response to the input parameters θ , a network Ψ processes θ and time t to generate parameters for an *output distribution*:

$$p_O(\mathbf{x}|\theta, t) = \prod_{d=1}^D p_O(x^{(d)}|\Psi^{(d)}(\theta, t)). \quad (3)$$

It is worth noting that each $p_I(x^{(d)}|\theta^{(d)})$ relies exclusively on information sampled through $p_S(y^{(d)}|x^{(d)}; \alpha)$, whereas each $p_O(x^{(d)}|\Psi^{(d)}(\theta, t))$ is contingent upon θ and consequently on \mathbf{x} . As a result, the output distribution possess the capability to leverage context information, in contrast to the input distribution.

Since receiver is aware of the sender distribution $p_S(\cdot|\mathbf{x}; \alpha)$ but lacks knowledge of \mathbf{x} , it consequently marginalizes over all possible data \mathbf{x}' , weighted by probabilities derived from the output distribution $p_O(\mathbf{x}|\theta, t)$. Therefore, we define the *receiver distribution* as:

$$p_R(\mathbf{y}|\theta; t, \alpha) = \mathbb{E}_{p_O(\mathbf{x}'|\theta, t)} p_S(\mathbf{y}|\mathbf{x}'; \alpha). \quad (4)$$

The transition from the prior distribution at $t = 0$ to the data-informed distribution at $t = 1$ is governed by a Bayesian flow. At each infinitesimal time step, given parameters θ and sender samples Y obtained with precision α , the *Bayesian update function* is derived by applying the principles of Bayesian inference to compute the updated parameters θ' :

$$\theta' \leftarrow h(\theta, \mathbf{y}, \alpha). \quad (5)$$

Consequently, to marginalize over \mathbf{y} , the *Bayesian update distribution* $p_U(\cdot|\theta, \mathbf{x}; \alpha)$ is defined as follows:

$$p_U(\theta'|\theta, \mathbf{x}; \alpha) = \mathbb{E}_{p_S(\mathbf{y}|\mathbf{x}; \alpha)} \delta(\theta' - h(\theta, \mathbf{y}, \alpha)), \quad (6)$$

where $\delta(\cdot)$ represents the Dirac delta distribution. As demonstrated before (Graves et al. 2023), accuracies expressed in the form of $p_U(\cdot|\theta, \mathbf{G}; \alpha)$ are additive. Therefore, Bayesian update distribution derived from prior parameters θ_0 can be formulated as follows:

$$p_U\left(\theta_n|\theta_0, \mathbf{G}; \sum_{i=1}^n \alpha_i\right) = \prod_{i=1}^{n-1} p_U(\theta_i|\theta_{i-1}, \mathbf{G}; \alpha_i) \mathbb{E} \left[p_U(\theta_n|\theta_{n-1}, \mathbf{G}; \alpha_n) \right]. \quad (7)$$

Integrating the Bayesian updates over time from prior parameters θ_0 gives rise to the formulation *Bayesian flow distribution*:

$$p_F(\theta|\mathbf{x}, t) = p_U(\theta|\theta_0, \mathbf{x}, \beta(t)). \quad (8)$$

This distribution characterizes the probability of observing parameters θ at time t , given the true data \mathbf{x} .

Methodology

We propose GraphBFN, a hierarchical framework for generative modeling of molecular graphs. Unlike previous work on BFNs focusing on discrete data within the probability simplex, our approach reformulates graph generation as a challenge situated in continuous-flow problem. Fig. 2 illustrates the overall framework of GraphBFN.

Hierarchical Coarse-to-Fine Framework

To effectively capture both local atomic connectivity and global molecular topology, GraphBFN integrates a hierarchical coarse-to-fine scheme inspired by the U-Net architecture (Ronneberger, Fischer, and Brox 2015), thereby constructing a multi-scale pyramid of graph representations. This methodology enables the model to initially generate a low-resolution structural scaffold, which is then refined progressively into a full-atom graph.

Coarse-to-Fine Generative Flow. The generative process unfolds in a coarse-to-fine manner, commencing with the coarsest graph at the bottleneck of the hierarchy without any conditional input. Along with the core neural network $\Psi^{(l)}$ in each BFN module at l -th layer, we define corresponding up-sampling module $\phi_1^{(l)}$ which takes as input the output from $\Psi^{(l)}$ and generates condition $\mathbf{c}^{(l)}$ for the following finer network $\Psi^{(l-1)}$:

$$\mathbf{c}^{(l)} = \Psi(\theta, \mathbf{c}^{(l+1)}, t). \quad (9)$$

The ensuing refinement process advances through the levels of the pyramid. At each finer scale, a BFN module generates a higher-resolution graph. The features generated at the coarser levels provide critical structural context for the refinement at finer levels, enabling GraphBFN to maintain and elaborate upon the global topology established at coarse levels during the fine-grained generation of both atomic and adjacent details.

Multi-Scale Loss Function. The model is trained in an end-to-end manner by optimizing a composite loss function, composed of the BFN generation loss \mathcal{L}_{BFN} and the differentiable pooling loss $\mathcal{L}_{\text{Pool}}$. The calculation of \mathcal{L}_{BFN} occurs at every scale of the pyramid, as elaborated in the subsequent section. Meanwhile, $\mathcal{L}_{\text{Pool}}$ is accumulated from all coarsening blocks. The final objective is defined as below:

$$\mathcal{L}_{\text{total}} = \mathcal{L}_{\text{BFN}} + \lambda_1 \sum_{l=0}^L \mathcal{L}_{\text{Pool}}^{(l)}, \quad (10)$$

where λ_1 serves as a hyperparameter balancing the two loss terms. This multi-scale objective ensures that the model not only learns to generate valid molecular structures but also acquires a meaningful hierarchical representation and modeling approach for them.

Graph Representation

Since manipulating discrete data often leads to more complex operations to guarantee differentiability, a foundational step of our method involves mapping the discrete atom and bond features into continuous spaces. For an attribute class $k \in \{0, \dots, K-1\}$, we define a deterministic mapping to a continuous value $x_k \in [-1, 1]$:

$$\begin{cases} k_c = \frac{2k+1}{K} - 1, \\ k_l = k_c - \frac{1}{K}, \\ k_r = k_c + \frac{1}{K}, \end{cases} \quad (11)$$

where k_l , k_c and k_r represent the corresponding vectors for left boundaries, centers and right boundaries of the bins. This mapping transforms the ground-truth graph \mathcal{G} into its continuous representation $\mathbf{G} = (\mathbf{X}, \mathbf{A})$, where each element of both \mathbf{X} and \mathbf{A} is a real number within the category $[\frac{1}{K} - 1, 1 - \frac{1}{K}]$. This continuous representation serves as the target for our generative flow.

Bayesian Flow Networks for Molecular Graphs

Input and Sender Distributions We model atom and bond features independently in the input distribution, using a set of parameters $\theta = \{\theta_X, \theta_A\}$. Each parameter set comprises a mean and a precision, specifically defined as $\theta \stackrel{\text{def}}{=} (\mu, \rho)$. The input priors are defined as:

$$p_I(\mathbf{X}|\theta_X) = \mathcal{N}(\mathbf{X}|\mu_X, \rho_X^{-1} \mathbf{I}), \quad (12)$$

$$p_I(\mathbf{A}|\theta_A) = \mathcal{N}(\mathbf{A}|\mu_A, \rho_A^{-1} \mathbf{I}), \quad (13)$$

where \mathbf{I} is the $D \times D$ identity matrix. The process initiates with a standard normal prior $p_I(\cdot|\theta_0) = \mathcal{N}(\cdot|\mathbf{0}, \mathbf{I})$ at time $t = 0$. These two equations can be integrated into: $p_I(\mathbf{G}|\theta) = \mathcal{N}(\mathbf{G}|\mu, \rho^{-1} \mathbf{I})$. For simplicity, we will use the integrated form of \mathbf{G} in our formulas, except in special circumstances.

Similarly, the noisy messages \mathbf{Y} are sampled from the sender distribution of \mathbf{G} according to Eq. 2:

$$p_S(\mathbf{Y}|\mathbf{G}; \alpha) = \mathcal{N}(\mathbf{Y}|\mathbf{G}, \alpha^{-1} \mathbf{I}). \quad (14)$$

Output and Receiver Distribution For discrete data, the output of core neural network $\epsilon = \Psi(\theta, \mathbf{c}, t)$ predicts the Gaussian noise vector ϵ used to generate the mean sample μ passed as input to Ψ . Specifically, $\Psi(\theta, \mathbf{c}, t)$ is converted into two D -length vectors, namely μ_ϵ and $\ln \sigma_\epsilon$, which are transformed into μ_x and σ_x using:

$$\mu_x = \begin{cases} 0 & \text{if } t < t_{\min}, \\ \frac{\mu}{\gamma(t)} - \sqrt{\frac{1 - \gamma(t)}{\gamma(t)}} \mu_\epsilon & \text{otherwise,} \end{cases} \quad (15)$$

$$\sigma_x = \begin{cases} 1 & \text{if } t < t_{\min}, \\ \sqrt{\frac{1 - \gamma(t)}{\gamma(t)}} \exp(\ln \sigma_\epsilon) & \text{otherwise,} \end{cases}$$

where $\gamma(t) = \beta(t)/(1 + \beta(t)) = 1 - \sigma_1^{2t}$ and $t_{\min} = 10^{-5}$.

Although we have successfully obtained μ_x, σ_x , they remain as parameters of a continuous Gaussian distribution. At this stage, we innovatively introduce CDF to compute the discrete probability distribution across each category. Consequently, the probability assigned to a specific category by the output distribution equals the function value at the right endpoint of CDF minus the function value at the left endpoint. Furthermore, since we utilize a limited continuous space to represent discrete data, the CDF equation needs to be truncated. Specifically, let the modified CDF of each dimension component be $\mathcal{F}(x|\mu_x^{(d)}, \sigma_x^{(d)})$, $d \in \{1, D\}$, then:

$$\mathcal{F}(x|\mu_x^{(d)}, \sigma_x^{(d)}) = \begin{cases} 0 & \text{if } x \leq -1, \\ 1 & \text{if } x \geq 1, \\ F(x|\mu_x^{(d)}, \sigma_x^{(d)}) & \text{otherwise,} \end{cases} \quad (16)$$

$$F(x|\mu_x^{(d)}, \sigma_x^{(d)}) = \frac{1}{2} \left[1 + \text{erf} \left(\frac{x - \mu_x^{(d)}}{\sqrt{2}\sigma_x^{(d)}} \right) \right], \quad (17)$$

where $F(\cdot)$ is the original CDF. The introduction of CDF effectively establishes a connection between discrete data and continuous distribution, thereby ensuring the continuous differentiability of the entire training process while retaining the inherent discrete characteristics of the data.

As a consequence, the probability for any discrete class $k \in \{0, K-1\}^D$ is computed by integrating this Gaussian's density over the corresponding continuous bin $[k_l, k_r]$:

$$p_O^{(d)}(k|\theta_x; t) = \mathcal{F}(k_r|\mu_x^{(d)}, \sigma_x^{(d)}) - \mathcal{F}(k_l|\mu_x^{(d)}, \sigma_x^{(d)}). \quad (18)$$

Differently, since the coarsened graphs $\tilde{\mathbf{G}}$ with parameters $\tilde{\theta}$ are in continuous states, graph mapping operation is no longer needed. Here ϵ is directly transformed into $\hat{\mathbf{x}}(\theta, t)$ to estimate \mathbf{x} :

$$\hat{\mathbf{x}}(\theta, t) = \frac{\mu}{\gamma(t)} - \sqrt{\frac{1 - \gamma(t)}{\gamma(t)}} \epsilon. \quad (19)$$

With relevant variables substituted into Eq. 3, we yield the output distributions of \mathbf{G} and $\tilde{\mathbf{G}}$:

$$\begin{cases} p_O(\mathbf{G}|\theta, t) = \prod_{d=1}^D p_O^{(d)}(k(G^{(d)})|\theta; t), \\ p_O(\tilde{\mathbf{G}}|\tilde{\theta}, t) = \delta(\tilde{\mathbf{G}} - \hat{\mathbf{G}}(\tilde{\theta}, t)). \end{cases} \quad (20)$$

Substituting Eqs. 20 and 2 into Eq. 4, respectively, we obtain the receiver distributions:

$$\begin{cases} p_R(\mathbf{Y}|\theta; t, \alpha) = \mathbb{E}_{p_O(\mathbf{G}'|\theta, t)} p_S(\mathbf{Y}|\mathbf{G}'; \alpha), \\ = \prod_{d=1}^D \sum_{k=0}^{K-1} p_O^{(d)}(k|\theta; t) \mathcal{N}(Y^{(d)}|k_c, \alpha^{-1}), \\ p_R(\tilde{\mathbf{Y}}|\tilde{\theta}; t, \alpha) = \mathcal{N}(\tilde{\mathbf{Y}}|\hat{\mathbf{G}}(\tilde{\theta}, t), \alpha^{-1} \mathbf{I}). \end{cases} \quad (21)$$

Bayesian Update Function Since both $p_I(\mathbf{G}|\theta)$ and $p_S(\mathbf{Y}|\mathbf{G}; \alpha)$ distributions are normal with diagonal covariance, a Bayesian posterior can be derived based on these prior distributions (Murphy 2007):

$$\begin{cases} h(\{\mu_{i-1}, \rho_{i-1}\}, \mathbf{Y}, \alpha) = \{\mu_i, \rho_i\}, \\ \rho_i = \rho_{i-1} + \alpha, \\ \mu_i = \frac{\mu_{i-1}\rho_{i-1} + \alpha\mathbf{Y}}{\rho_i}. \end{cases} \quad (22)$$

BFN Loss Function

We train our model utilizing a continuous-time loss formulation, which offers a stable and efficient objective. For discrete data \mathbf{G} , the loss is the expected squared error between the target continuous data and the expected value of the discretized output distribution, weighted by the accuracy rate. The expected value of the discretized output distribution for a given attribute is:

$$\hat{k}(\theta, t) = \mathbb{E}[p_O(\cdot|\theta, t)] = \text{NEAREST_CENTER}(\theta, t) = \left(\sum_{k=0}^{K-1} k_c \cdot p_O^{(1)}(k|\theta, t), \dots, \sum_{k=0}^{K-1} k_c \cdot p_O^{(D)}(k|\theta, t) \right), \quad (23)$$

where k_c is the center of the k -th bin, and the function **NEAREST_CENTER** compares inputs to these center bins $\hat{k}_c = (k_c^{(1)}, \dots, k_c^{(D)})$ to identify their nearest counterparts. The total loss for a graph \mathbf{G} is the sum of losses for its atom and bond features:

$$\mathcal{L}_{\mathbf{G}} = \mathcal{L}_{\mathbf{X}} + \mathcal{L}_{\mathbf{A}}, \quad (24)$$

where the loss for the atom features is expressed as follows:

$$\mathcal{L}_{\mathbf{X}} = -\ln \sigma_1 \mathbb{E}_{t \sim U(0,1), \theta \sim p_F(\theta|\mathbf{X}; t)} \frac{\|\mathbf{X} - \hat{k}_{\mathbf{cX}}(\theta, t)\|^2}{\sigma_1^{2t}}, \quad (25)$$

and a similar expression applies for $\mathcal{L}_{\mathbf{A}}(\mathbf{A})$. Differently, for continuous data $\tilde{\mathbf{G}}$, the loss is directly calculated by:

$$\mathcal{L}_{\tilde{\mathbf{G}}} = -\ln \sigma_1 \mathbb{E}_{t \sim U(0,1), p_F(\theta|\tilde{\mathbf{G}}; t)} \frac{\|\tilde{\mathbf{G}} - \hat{\mathbf{G}}(\tilde{\theta}, t)\|^2}{\sigma_1^{2t}}. \quad (26)$$

And the final BFN loss is derived as follows:

$$\mathcal{L}_{\text{BFN}} = \mathcal{L}_{\mathbf{G}} + \lambda_2 \sum_{l=0}^L \mathcal{L}_{\tilde{\mathbf{G}}}^{(l)}, \quad (27)$$

where λ_2 serves as a hyperparameter that balances the two loss components.

Method	QM9				ZINC250k				Sampling Steps
	Val. w/o corr. \uparrow	Unique \uparrow	FCD \downarrow	NSPDK \downarrow	Val. w/o corr. \uparrow	Unique \uparrow	FCD \downarrow	NSPDK \downarrow	
MoFlow	91.36	98.65	4.467	0.0169	63.76	99.99	20.875	0.0468	-
EDP-GNN	47.52	99.25	2.68	0.0052	83.16	99.79	16.819	0.0483	1000
GraphEBM	8.22	97.90	6.143	0.0287	5.29	98.79	35.467	0.2089	-
GDSS	95.72	98.46	2.565	0.0033	97.12	99.64	14.032	0.0192	1000
DiGress	99.00	96.20	-	-	94.98	99.21	-	-	500
GSDM	99.90	-	2.614	0.0034	92.57	-	12.435	0.0168	1000
Dirichlet FM	99.10	98.15	0.888	0.0041	97.52	99.20	14.222	0.0328	400
CatFlow	99.81	99.95	0.441	0.0029	99.21	100.00	13.211	0.0207	-
GraphBFN _{w/o}	99.50	99.09	0.326	0.0015	94.81	100.00	6.120	0.0095	100
GraphBFN	99.60	99.97	0.214	0.0008	96.00	100.00	5.743	0.0069	$100 \times L$

Table 1: Generation results on QM9 and ZINC250k datasets. The best results are highlighted in bold. Val. w/o corr. denotes validity without correction metric. GraphBFN_{w/o} generates molecular graphs without hierarchical supervision for ablation study. Null values in criteria indicate that statistics are unavailable from the original paper. MoFlow and GraphEBM are one-shot models, hence lack of sampling steps. And CatFlow employs a solver with adaptive step size control, resulting in a non-fixed step size.

Generative Sampling

To sample a new graph, we reverse the generative process by initiating with parameters for a simple prior and iteratively refining them over T time steps. Algorithm 1 illustrates the sampling procedure, wherein the function PRED is implemented based on the derivation of the output distribution.

Algorithm 1: Sampling Algorithm

Require: $\sigma_{1_X}, \sigma_{1_A} \in \mathbb{R}^+$, number of steps $n, K_X, K_A \in \mathbb{N}$
 $\mathbf{c} \leftarrow \text{None}$
for $l = L$ to 0 **do**
 $\mu_X, \mu_A \leftarrow 0$
 $\rho_X, \rho_A \leftarrow 1$
 for $i = 1$ to n **do**
 $t \leftarrow \frac{i}{n}$
 $\gamma_X, \gamma_A \leftarrow 1 - \sigma_{1_X}^{2t}, 1 - \sigma_{1_A}^{2t}$
 $p_{O_X}(\cdot | \theta_X, t), p_{O_A}(\cdot | \theta_A, t) \leftarrow \text{PRED}(\mu_X, \mu_A, t, K_X, K_A, \gamma_X, \gamma_A, \mathbf{c})$
 $\alpha_X, \alpha_A \leftarrow \sigma_{1_X}^{-2i/n} (1 - \sigma_{1_X}^{2/n}), \sigma_{1_A}^{-2i/n} (1 - \sigma_{1_A}^{2/n})$
 $\mathbf{y}_X \sim \mathcal{N}(k_{c_X}, \alpha_X^{-1} I)$
 $\mathbf{y}_A \sim \mathcal{N}(k_{c_A}, \alpha_A^{-1} I)$
 $\mu_X, \mu_A \leftarrow \frac{\rho_X \mu_X + \alpha_X \mathbf{y}_X}{\rho_X + \alpha_X}, \frac{\rho_A \mu_A + \alpha_A \mathbf{y}_A}{\rho_A + \alpha_A}$
 $\rho_X, \rho_A \leftarrow \rho_X + \alpha_X, \rho_A + \alpha_A$
 end for
 $p_{O_X}(\cdot | \theta_X, t), p_{O_A}(\cdot | \theta_A, t), \mathbf{c} \leftarrow \text{PRED}(\mu_X, \mu_A, 1, K_X, K_A, 1 - \sigma_{1_X}^2, 1 - \sigma_{1_A}^2, \mathbf{c})$
end for
 $\hat{k}_{c_X}(\theta_X, 1) \leftarrow \text{NEAREST_CENTER}(\theta_X, 1)$
 $\hat{k}_{c_A}(\theta_A, 1) \leftarrow \text{NEAREST_CENTER}(\theta_A, 1)$
return $\hat{k}_{c_X}(\theta_X, 1), \hat{k}_{c_A}(\theta_A, 1)$

Experiment

We experimentally validate the performance of our method in molecular graph generation task as well as sampling efficiency comparison against representative baselines.

Experimental Setup

Dataset We choose QM9 (Ramakrishnan et al. 2014) and ZINC250k (Irwin et al. 2012) for molecular graph generation, where QM9 consists of small and ZINC250k includes relatively large molecules.

Evaluation Metrics We evaluate the quality of 10,000 generated molecules with validity without correction metrics and uniqueness. Fréchet ChemNet Distance (FCD) (Preuer et al. 2018) measures the distance between training and generated sets using the activations from the penultimate layer of the ChemNet. Additionally, Neighborhood Subgraph Pairwise Distance Kernel (NSPDK) maximum mean discrepancy (MMD) (Costa and De Grave 2010) evaluates the MMD between the generated molecules and test molecules which takes into account both the atom and bond features for evaluation.

Baselines We compare our model against several state-of-the-art baselines in graph generation. MoFlow (Zang and Wang 2020) is a one-shot flow-based model. EDP-GNN (Niu et al. 2020) models graphs with a permutation invariant approach. GraphEBM (Liu et al. 2021) generates molecules by minimizing energies with Langevin dynamics. GDSS (Jo, Lee, and Hwang 2022) is a score-based diffusion model. DiGress (Vignac et al. 2023) generates graphs using a discrete diffusion process. GSDM (Luo, Mo, and Pan 2023) operates on the graph spectrum space by low-rank diffusion stochastic differential equations (SDEs). Dirichlet FM (Stark et al. 2024) is a distilled Dirichlet flow matching method. Cat-

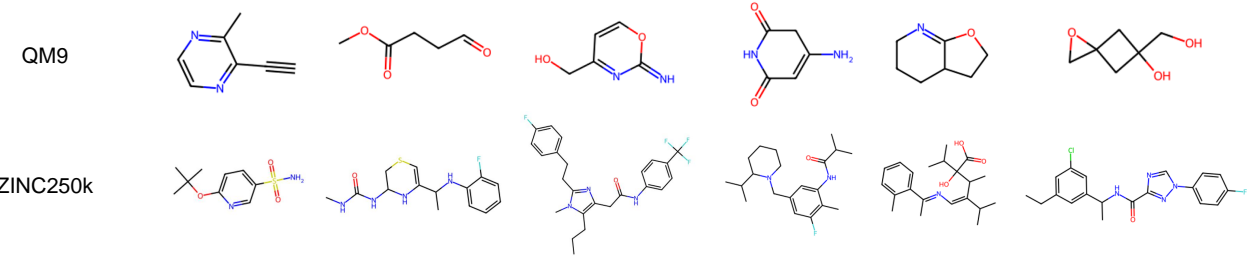


Figure 3: Samples generated by GraphBFN on ZINC250K and QM9 datasets.

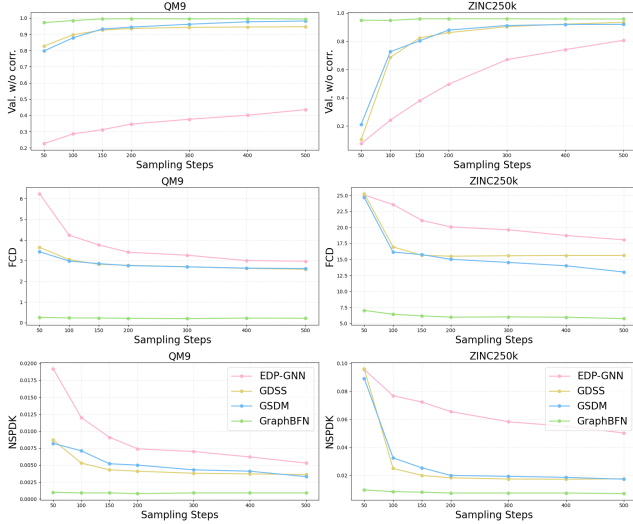


Figure 4: Sampling efficiency as a measure of the quality of inference time with respect to sampling steps on QM9 and ZINC250k.

Flow (Eijkelboom et al. 2024) is a variational flow matching method for categorical data.

Molecular Graph Generation

In our experiments, GraphBFN demonstrates superior performance on both QM9 and ZINC250k. As shown in Table. 1, our model achieves new state-of-the-art results for uniqueness, FCD, and NSPDK, outperforming previous flow-based, flow matching, and diffusion models. Specifically, 51.5% and 72.4% improvements on FCD and NSPDK indicate the molecules generated by GraphBFN closely align with the distributions of the relevant molecular datasets. Furthermore, the highest score on uniqueness manifests the best diversity performance and exploration capability during generation, which further highlights the deficiency of the methods regarding the training objective as a regression task in terms of molecular diversity. Since all methods attain 100% validity after molecular correction, GraphBFN maintains a leading position on this metric. Additionally, Table. 1 reveals that GraphBFN can achieve SOTA effects with significantly fewer sampling steps. We also present randomly selected molecular samples in Fig. 3 for visualization. This

compelling empirical evidence highlights the effectiveness of our work, facilitating rapid generation of higher-fidelity and more diverse molecular graphs.

Sampling Efficiency and Effect

We conduct a sampling efficiency experiment to compare the sampling velocity against representative baselines. Given that the sampling steps of GraphBFN are influenced by the parameter L , we utilize GraphBFN_{w/o} in this comparison for fairness. As manifested in Fig. 4, our method exhibits exceptional performance during the initial 50 steps, and our scores could be further improved if sampling sufficiently with longer steps. This characteristic renders GraphBFN well-suited for generating high-quality molecular samples while maintaining competitive in inference time.

Ablation Study

We performed an ablation study to assess the effectiveness of the hierarchical coarse-to-fine framework in enhancing BFN. As shown in Table. 1, GraphBFN outperforms GraphBFN_{w/o} across all evaluation criteria. Although a certain degree of sampling speed is sacrificed, we reckon that this framework equips GraphBFN with molecular structure information at various scales and offers accurate and effective guidance during sampling process from different granularities.

Conclusion

In this paper, we introduce GraphBFN, a novel hierarchical coarse-to-fine BFN framework for molecular graph generation that adapts the principles of Bayesian Flow Networks in a new paradigm. By fully utilizing data distribution parameters, we innovatively introduce CDF to calculate the probabilities of various categories instead of overfitting to specific numerical values, which unifies the training objective and sampling rounding operation. Our approach achieves state-of-the-art performance on challenging molecular graph generation benchmarks, demonstrating its capability to produce high-quality and diverse molecular graphs. However, our interpretability analysis regarding how multi-scale information optimizes generation results is insufficient. In future work, we will explore the application of GraphBFN to larger and more complex graph domains, investigate its potential for conditional generation tasks, and enhance the interpretability analysis.

References

Chen, J.; Cai, X.; Wu, J.; and Hu, W. 2025. Antibody Design and Optimization with Multi-scale Equivariant Graph Diffusion Models for Accurate Complex Antigen Binding. *arXiv preprint arXiv:2506.20957*.

Costa, F.; and De Grave, K. 2010. Fast neighborhood subgraph pairwise distance kernel. In *Proceedings of the 26th International Conference on Machine Learning*, 255–262. Omnipress; Madison, WI, USA.

De Cao, N.; and Kipf, T. 2018. MolGAN: An implicit generative model for small molecular graphs. *ICML 2018 workshop on Theoretical Foundations and Applications of Deep Generative Models*.

Eijkelboom, F.; Bartosh, G.; Andersson Naesseth, C.; Welling, M.; and van de Meent, J.-W. 2024. Variational flow matching for graph generation. *Advances in Neural Information Processing Systems*, 37: 11735–11764.

Gong, H.; Liu, Q.; Wu, S.; and Wang, L. 2024. Text-guided molecule generation with diffusion language model. In *Proceedings of the AAAI Conference on Artificial Intelligence*, volume 38, 109–117.

Graves, A.; Srivastava, R. K.; Atkinson, T.; and Gomez, F. 2023. Bayesian flow networks. *arXiv preprint arXiv:2308.07037*.

Huang, H.; Sun, L.; Du, B.; Fu, Y.; and Lv, W. 2022. Graphgdp: Generative diffusion processes for permutation invariant graph generation. In *2022 IEEE International Conference on Data Mining (ICDM)*, 201–210. IEEE.

Irwin, J. J.; Sterling, T.; Mysinger, M. M.; Bolstad, E. S.; and Coleman, R. G. 2012. ZINC: a free tool to discover chemistry for biology. *Journal of chemical information and modeling*, 52(7): 1757–1768.

Jin, W.; Barzilay, R.; and Jaakkola, T. 2018. Junction tree variational autoencoder for molecular graph generation. In *International conference on machine learning*, 2323–2332. PMLR.

Jin, W.; Barzilay, R.; and Jaakkola, T. 2020. Hierarchical generation of molecular graphs using structural motifs. In *International conference on machine learning*, 4839–4848. PMLR.

Jo, J.; Lee, S.; and Hwang, S. J. 2022. Score-based generative modeling of graphs via the system of stochastic differential equations. In *International conference on machine learning*, 10362–10383. PMLR.

Kong, X.; Huang, W.; Tan, Z.; and Liu, Y. 2022. Molecule generation by principal subgraph mining and assembling. *Advances in Neural Information Processing Systems*, 35: 2550–2563.

Lee, S.; Jo, J.; and Hwang, S. J. 2023. Exploring chemical space with score-based out-of-distribution generation. In *International Conference on Machine Learning*, 18872–18892. PMLR.

Li, K.; Gong, X.; Pan, S.; Wu, J.; Du, B.; and Hu, W. 2024. Regressor-free molecule generation to support drug response prediction. *arXiv preprint arXiv:2405.14536*.

Li, K.; Xiong, Y.; Zhang, H.; Cai, X.; Wu, J.; Du, B.; and Hu, W. 2025a. Graph-structured Small Molecule Drug Discovery Through Deep Learning: Progress, Challenges, and Opportunities. *arXiv preprint arXiv:2502.08975*.

Li, K.; Zeng, Y.; Xiong, Y.-d.; Wu, H.-c.; Fang, S.; Qu, Z.-y.; Zhu, Y.; Du, B.; Gao, Z.-b.; and Hu, W.-b. 2025b. Contrastive learning-based drug screening model for GluN1/GluN3A inhibitors. *Acta Pharmacologica Sinica*, 1–13.

Liu, C.; Fan, W.; Liu, Y.; Li, J.; Li, H.; Liu, H.; Tang, J.; and Li, Q. 2023. Generative diffusion models on graphs: methods and applications. In *Proceedings of the Thirty-Second International Joint Conference on Artificial Intelligence*, 6702–6711.

Liu, M.; Yan, K.; Oztekin, B.; and Ji, S. 2021. GraphEBM: Molecular Graph Generation with Energy-Based Models. In *Energy Based Models Workshop-ICLR 2021*.

Luo, T.; Mo, Z.; and Pan, S. J. 2023. Fast graph generation via spectral diffusion. *IEEE Transactions on Pattern Analysis and Machine Intelligence*, 46(5): 3496–3508.

Luo, Y.; Yan, K.; and Ji, S. 2021. Graphdf: A discrete flow model for molecular graph generation. In *International conference on machine learning*, 7192–7203. PMLR.

Martinkus, K.; Loukas, A.; Perraudeau, N.; and Wattenhofer, R. 2022. Spectre: Spectral conditioning helps to overcome the expressivity limits of one-shot graph generators. In *International Conference on Machine Learning*, 15159–15179. PMLR.

Murphy, K. P. 2007. Conjugate Bayesian analysis of the Gaussian distribution. *def*, 1(2 σ 2): 16.

Niu, C.; Song, Y.; Song, J.; Zhao, S.; Grover, A.; and Ermon, S. 2020. Permutation invariant graph generation via score-based generative modeling. In *International conference on artificial intelligence and statistics*, 4474–4484. PMLR.

Preuer, K.; Renz, P.; Unterthiner, T.; Hochreiter, S.; and Klambauer, G. 2018. Fréchet ChemNet distance: a metric for generative models for molecules in drug discovery. *Journal of chemical information and modeling*, 58(9): 1736–1741.

Qiu, R.; Wang, D.; Ying, L.; Poor, H. V.; Zhang, Y.; and Tong, H. 2023. Reconstructing graph diffusion history from a single snapshot. In *Proceedings of the 29th ACM SIGKDD Conference on Knowledge Discovery and Data Mining*, 1978–1988.

Qu, Y.; Qiu, K.; Song, Y.; Gong, J.; Han, J.; Zheng, M.; Zhou, H.; and Ma, W.-Y. 2024. MolCRAFT: Structure-Based Drug Design in Continuous Parameter Space. In *Forty-first International Conference on Machine Learning*.

Ramakrishnan, R.; Dral, P. O.; Rupp, M.; and Von Lilienfeld, O. A. 2014. Quantum chemistry structures and properties of 134 kilo molecules. *Scientific data*, 1(1): 1–7.

Ronneberger, O.; Fischer, P.; and Brox, T. 2015. U-net: Convolutional networks for biomedical image segmentation. In *International Conference on Medical image computing and computer-assisted intervention*, 234–241. Springer.

Shi, C.; Xu, M.; Zhu, Z.; Zhang, W.; Zhang, M.; and Tang, J. 2020. GraphAF: a Flow-based Autoregressive Model for Molecular Graph Generation. In *International Conference on Learning Representations*.

Simonovsky, M.; and Komodakis, N. 2018. Graphvae: Towards generation of small graphs using variational autoencoders. In *International conference on artificial neural networks*, 412–422. Springer.

Song, Y.; Gong, J.; Zhou, H.; Zheng, M.; Liu, J.; and Ma, W.-Y. 2024. Unified generative modeling of 3d molecules with bayesian flow networks. In *The Twelfth International Conference on Learning Representations*.

Stark, H.; Jing, B.; Wang, C.; Corso, G.; Berger, B.; Barzilay, R.; and Jaakkola, T. 2024. Dirichlet flow matching with applications to DNA sequence design. In *Proceedings of the 41st International Conference on Machine Learning*, 46495–46513.

Vignac, C.; Krawczuk, I.; Siraudin, A.; Wang, B.; Cevher, V.; and Frossard, P. 2023. DiGress: Discrete Denoising diffusion for graph generation. In *The Eleventh International Conference on Learning Representations*.

Wu, L.; Huang, Y.; Tan, C.; Gao, Z.; Hu, B.; Lin, H.; Liu, Z.; and Li, S. Z. 2024. Psc-cpi: Multi-scale protein sequence-structure contrasting for efficient and generalizable compound-protein interaction prediction. In *Proceedings of the AAAI conference on artificial intelligence*, volume 38, 310–319.

Xiong, Y.; Li, K.; Chen, J.; Zhang, H.; Lin, D.; Che, Y.; and Hu, W. 2024. Text-guided multi-property molecular optimization with a diffusion language model. *arXiv preprint arXiv:2410.13597*.

Xu, Z.; Qiu, R.; Chen, Y.; Chen, H.; Fan, X.; Pan, M.; Zeng, Z.; Das, M.; and Tong, H. 2024. Discrete-state continuous-time diffusion for graph generation. *Advances in Neural Information Processing Systems*, 37: 79704–79740.

Ying, Z.; You, J.; Morris, C.; Ren, X.; Hamilton, W.; and Leskovec, J. 2018. Hierarchical graph representation learning with differentiable pooling. *Advances in neural information processing systems*, 31.

You, J.; Liu, B.; Ying, Z.; Pande, V.; and Leskovec, J. 2018a. Graph convolutional policy network for goal-directed molecular graph generation. *Advances in neural information processing systems*, 31.

You, J.; Ying, R.; Ren, X.; Hamilton, W.; and Leskovec, J. 2018b. Graphrnn: Generating realistic graphs with deep auto-regressive models. In *International conference on machine learning*, 5708–5717. PMLR.

Zang, C.; and Wang, F. 2020. Moflow: an invertible flow model for generating molecular graphs. In *Proceedings of the 26th ACM SIGKDD international conference on knowledge discovery & data mining*, 617–626.

Zhu, Y.; Wu, J.; Hu, C.; Yan, J.; Hou, T.; Wu, J.; et al. 2023. Sample-efficient multi-objective molecular optimization with gflownets. *Advances in Neural Information Processing Systems*, 36: 79667–79684.